IEEE Access
Multidisciplinary | Rapid Review | Open Access Journal

Received June 19, 2018, accepted July 20, 2018, date of publication July 26, 2018, date of current version August 20, 2018.

Digital Object Identifier 10.1109/ACCESS.2018.2860050

State of Charge Estimation of Lithium-Ion Batteries Over Wide Temperature Range Using Unscented Kalman Filter

XIAOGANG WU[1,2], XUEFENG LI[1], AND JIUYU DU[2]

[1]College of Electrical and Electronics Engineering, Harbin University of Science and Technology, Harbin 150080, China
[2]State Key Laboratory of Automotive Safety and Energy, Tsinghua University, Beijing 100084, China

Corresponding author: Jiuyu Du (dujiuyu@tsinghua.edu.cn)

This work was supported in part by the National Key Technologies Research and Development Program of MOST under Grant 2016YFB0101801, in part by the State Key Laboratory of Automotive Safety and Energy under Project KF1826, and in part by the University Nursing Program for Young Scholars with Creative Talents in Heilongjiang Province under Grant UNPYSCT-2016164.

ABSTRACT With the development of electric vehicles in recent years, lithium-ion batteries have been widely used. Accurate state of charge (SOC) estimation plays an important role in the safety of electric vehicles. Since the temperature has the significant influence on charge and discharge performance of the battery, it is critical to achieve accurate SOC estimation over the wide temperature range. In this paper, a polymer ternary lithium-ion battery is focused, and a Thevenin equivalent circuit model with temperature compensation is established. The validity of the established battery model was verified by the dynamic stress test. On this basis, the ternary lithium-ion battery SOC was estimated using the unscented Kalman filter (UKF). The New European Driving Cycle is used to verify the effectiveness of the proposed algorithm. The simulation and experimental results show that the established Thevenin equivalent circuit model with temperature compensation can accurately represent the battery dynamics. Based on this model, the SOC was estimated using the UKF and the maximum errors are within 3%. Therefore, the proposed SOC estimation method is verified to be effective and robust.

INDEX TERMS Lithium battery, temperature compensation, SOC estimation, unscented Kalman filter.

I. INTRODUCTION

As an energy storage device for electric vehicles (EV), hybrid electric vehicles (HEV) and fuel cell electric vehicles (FCEV), lithium-ion batteries require effective battery management methods to prolong the service life and improve reliability and safety [1]. Battery State of Charge (SOC) estimation is a hot issue in battery management research. Accurate estimation of battery SOC can prevent battery over-charge and over-discharge, reduce damage to the battery, improve battery performance, and therefore plays an important role in the battery management system [2], [3].

The existing studies related to battery SOC estimation mainly focus on battery model construction and the SOC estimation algorithm [4]. As for the battery model construction, He *et al*. [5] summarized a variety of equivalent circuit models, including the Rint model, the Thevenin model, the RC model, the DP model and the Partnership for a New Generation of Vehicles (PNGV) model. Reference [5] compared and analyzed the five equivalent circuit models, providing guidance for the selection and application of equivalent circuit models. Xiong *et al.* [6] used the electrochemical polarization Nernst model for battery parameter identification and estimated SOC of the battery used in plug-in hybrid vehicles. Tian *et al.* [7] proposed a new simpler modified equivalent circuit model to improve the model accuracy. Li *et al.* [8] established the third-order RC equivalent circuit model and Zhang *et al.* [9] established the Gaussian-based model of a lithium-ion battery. However, these two models are relatively complex. The battery model proposed by Roscher and Sauer [10] considering OCV recovery and hysteresis, and the maximum estimation error of SOC is within 2%.

As for the SOC estimation algorithms, Zhe *et al*. [11] applied SOC estimation with the initial SOC correction of the coulomb counting method to eliminate the SOC accumulation error. He *et al*. [12] compared the adaptive extended Kalman filter (AEKF) algorithm with the EKF algorithm to estimate the battery SOC in real-time, the AEKF

algorithm had a better performance than the EKF algorithm. Xiong Rui proposed a variety of methods to estimate battery SOC, which includes the method based on SEI impedance [13], double-scale particle filter [14], and a novel method was used to get the OCV-SOC relationship with low computational cost, which can keep SOC estimation error within 1% [15]. Yu *et al*. [16] proposed a joint SOC estimation method, and model parameters of battery are estimated online using the H-infinity filter, the SOC is estimated using the unscented Kalman filter. Shulin *et al*. [17] estimated the SOC based on the theory of fractional order model. In addition, some intelligent algorithms were also used in the estimation of battery SOC. Chaoui *et al*. [18] applied input time-delayed neural networks to estimate the battery SOC achieving estimated RMSE within 0.0033.

Above studies present a comprehensive investigation of battery SOC estimation methods and model construction, but the influence of temperature on the SOC estimation is seldom mentioned. There are significant changes in battery parameters such as battery capacity and open circuit voltage at different temperatures [19], [20]. In the literature [21], a temperature-compensated model was presented for power Li-ion batteries in EVs, and a dual-particle-filter estimator was used to estimate SOC. The temperature range considered by Lee KuanTing is 37°C to 40°C and does not extend over a wider temperature range [22]. Based on the Rint model, Xing *et al*. [23] considered the effect of temperature on the open circuit voltage and the internal resistance of the battery, but could not fully reflect the effect of temperature on the polarization effect. In order to make the battery SOC estimation robust to ambient temperature changes, this paper establishes the Thevenin equivalent circuit model with temperature compensation. Considering the battery temperature range from 0°C to 40°C, the battery capacity, open circuit voltage, ohm resistance, polarization resistance and polarization capacitance are tested and identified. The model is verified under the dynamic stress test (DST). Given that the coulomb counting method [24] has error accumulation, the open-circuit voltage method [25] takes a long time to stand still, the intelligent algorithm [26] requires long training time, and the estimated accuracy of the extended Kalman filter algorithm [27] reaches only first-order, the UKF algorithm is used in this paper to estimate the SOC.

II. BATTERY MODEL AND PARAMETER IDENTIFICATION

A. EQUIVALENT CIRCUIT MODEL

Currently, the battery models used in SOC estimation are mainly divided into several types: electrochemical model, neural network model and equivalent circuit model and so on. The equivalent circuit model, which is composed of resistance, capacitance, constant voltage source and other components, can simulate the battery dynamics. Among them, the equivalent circuit model is easier to identify the battery parameters, which is beneficial to engineering implementation [28]. The equivalent circuit model mainly includes the Rint model, the Thevenin model, the PNGV model and the GNL model and so on. The Thevenin circuit model is a good option for the equivalent circuit model due to the enough accuracy and low computational cost. Therefore, in this paper, the Thevenin circuit model is used [29], as shown in Fig. 1.

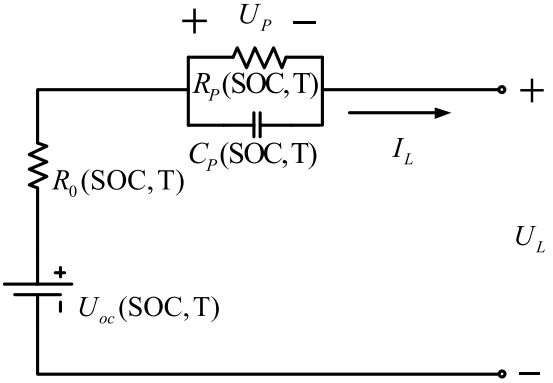

FIGURE 1. Thevenin equivalent circuit model.

In Fig. 1, U_{oc} is the open circuit voltage (V), R_0 is the ohm resistance, R_p is the polarization resistance, C_p is the polarization capacitor, U_p is the polarization voltage, $U_L U_L$is the terminal voltage t, andI_L is the load curren. The parameters in the equivalent circuit are affected by SOC and temperature (T).

The mathematical model of the circuit is described as(1).

$$\begin{cases} \dot{U_p} = -\dfrac{U_p}{R_p C_p} + \dfrac{I_L}{C_p} \\ U_L = U_{oc} - U_p - I_L R_0 \end{cases} \tag{1}$$

B. BATTERY PARAMETER IDENTIFICATION

The ohm resistance, polarization resistance and polarization capacitance are all affected by SOC and temperature. Therefore, the capacity and open circuit voltage must be tested and the battery parameters can be identified through HPPC test from 0°C to 40°C with an interval of 10°C.

A battery test bench was set up, which consists of battery test equipment, temperature chamber, temperature sensor and related software, as shown in Fig. 2.

The selected battery parameters are shown in Table 1.

TABLE 1. Table battery basic parameters.

Parameters (unit)	values
Rated Capacity (mAh)	2600
Nominal voltage (V)	3.6
Charge cut-off voltage(V)	4.2
Discharge cut-off voltage (V)	2.75
Battery mass (g)	45
Operating Temperature(°C)	0~45

1) AVAILABLE CAPACITY –T TEST

The battery available capacity test steps are as follows: (1) the battery is fully discharged with 1/3C current to achieve the

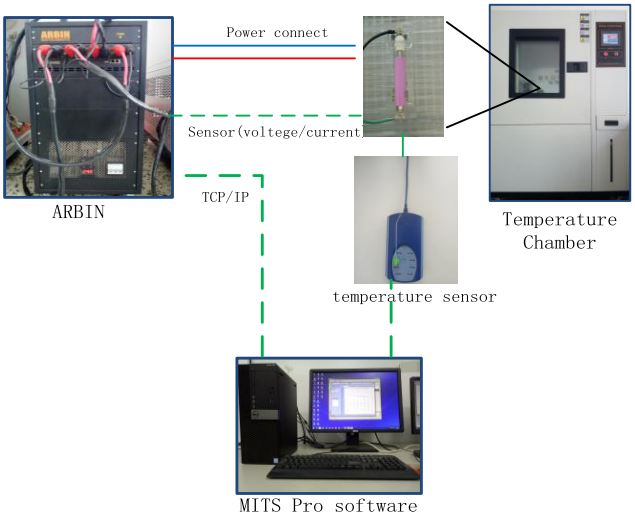

FIGURE 2. Battery test bench.

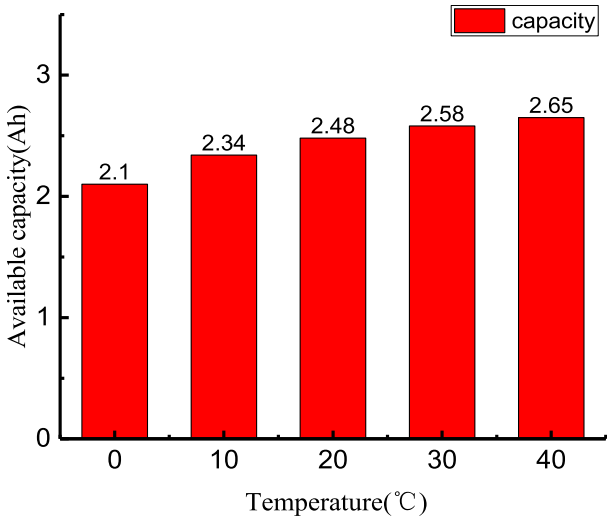

FIGURE 3. Battery available capacity at different temperatures.

discharge cut-off voltage of 2.75V, and has a rest of 1 hour. Note that the SOC is 0% at this time. (2) the cell is fully charged with 1/3C current to achieve the charge cut-off voltage of 4.2V, then constant voltage charging is conducted. When the current is less than 0.02C, the charging is completed, and the cell has a rest of 1 hour. Note that the SOC is 100% at this time. (3) step (1) and step (2) are repeated three times. Then take the average value of three discharge capacities as available capacity .If the error between the maximum discharge capacity value and the average capacity value is less than 2%, then the available capacity test is stopped and the average capacity value is considered as the available capacity; however, the battery available capacity test experiment continues with the above steps if the error exceeds 2% [30]. (4) In order to obtain the available battery capacity at different temperatures, the above steps are required to be repeated at 0°C to 40°C (10°C intervals). The available capacity of the battery is related to many factors. Different temperatures, C-rate and aging correspond to different available capacities [7]. In this paper, the effect of temperature on available capacity is considered, then the relationship between available capacity and temperature (Cap-T) is feasible and reasonable [22]. The experimental results are shown in Fig. 3. Fig. 3 shows that the effect of temperature on the battery available capacity is significant, and the battery available capacity increases as the temperature increases. At low temperatures, the available capacity significantly reduces. The available capacity reduces by 19.23% at 0°C when compared to the rated battery capacity.

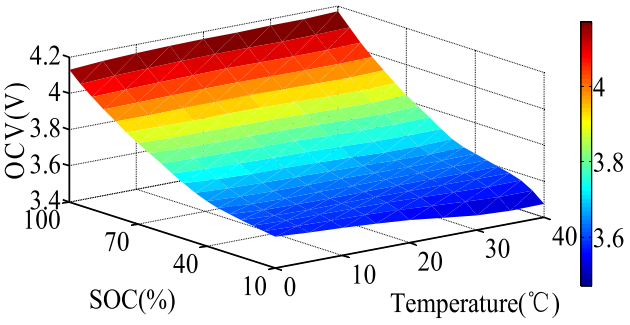

FIGURE 4. OCV-SOC-T.

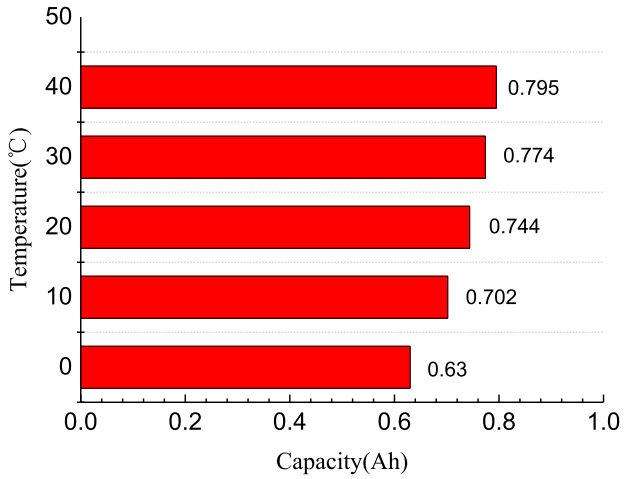

FIGURE 5. OCV = 3.6V, comparison of available battery capacity at different temperatures.

2) THE OCV-SOC-T TEST

This paper refers to the battery open circuit voltage test in [12] and obtains the OCV-SOC-T data, as shown in Fig. 4.

As shown in Fig.4, the battery OCV is not only related to the SOC, but also influenced by the temperature. As shown in literature [31], the OCV increases as the temperature increases. Fig.5 shows that at the same OCV (OCV = 3.60V), different temperatures correspond to different battery capacities, and the maximum available battery capacity differs by 0.165 Ah, which indicates the necessity of establishing a temperature compensation model.

2) HPPC test

The data of HPPC test is used to identify the battery parameters offline. When the ambient temperature is 20°C, the HPPC test curve is shown in Fig. 6.

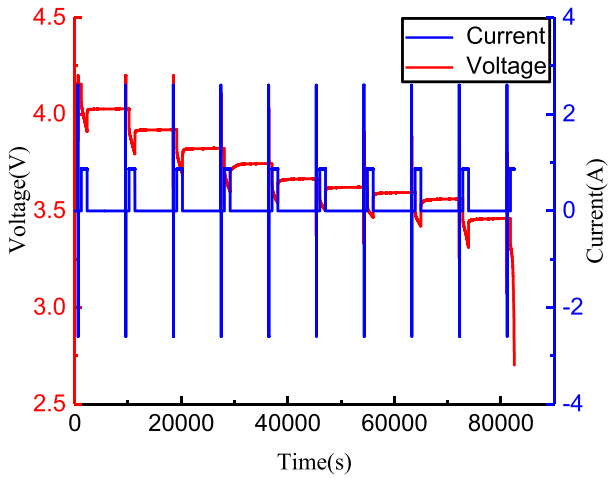

FIGURE 6. HPPC test curves.

In this paper, the Recursive Least Squares (RLS) [32] with forgetting factor is used to identify the parameters of Thevenin circuit model, and the battery parameters at different temperatures are shown in Fig.7.

Fig.7 shows the battery parameter identification results, and it can be concluded that the ohm resistance R_0 and the polarization resistance R_p increases as the temperature decreases, but the polarization capacitance C_p decreases as the temperature decreases. Considering 20°C as room temperature [33], [34], the corresponding battery parameters are used as the parameters of the conventional OCV-SOC model.

C. BATTERY MODEL VALIDATION

The model verification test was performed under DST to verify the accuracy of the Thevenin equivalent circuit model with temperature compensation [5]. This paper selects 10 cycles of DST for verification. The initial battery SOC is 100%. The DST current is shown in Fig. 8(a). Taking the ambient temperature 20°C as an example, the simulation voltage and the measurement are shown in Fig. 8(b).

Equivalent circuit model verification tests are performed with DST at five temperatures. The error of the estimated voltage is shown in Fig. 9. The mean absolute errors are listed in Table 2. The voltage error (e_t) and mean absolute error (MAE) defined in this paper are shown as (2) and (3),

TABLE 2. Table mean absolute error of voltage.

T (℃)	0	10	20	30	40
MAE	0.2958%	0.2829%	0.2076%	0.114%	0.2141%

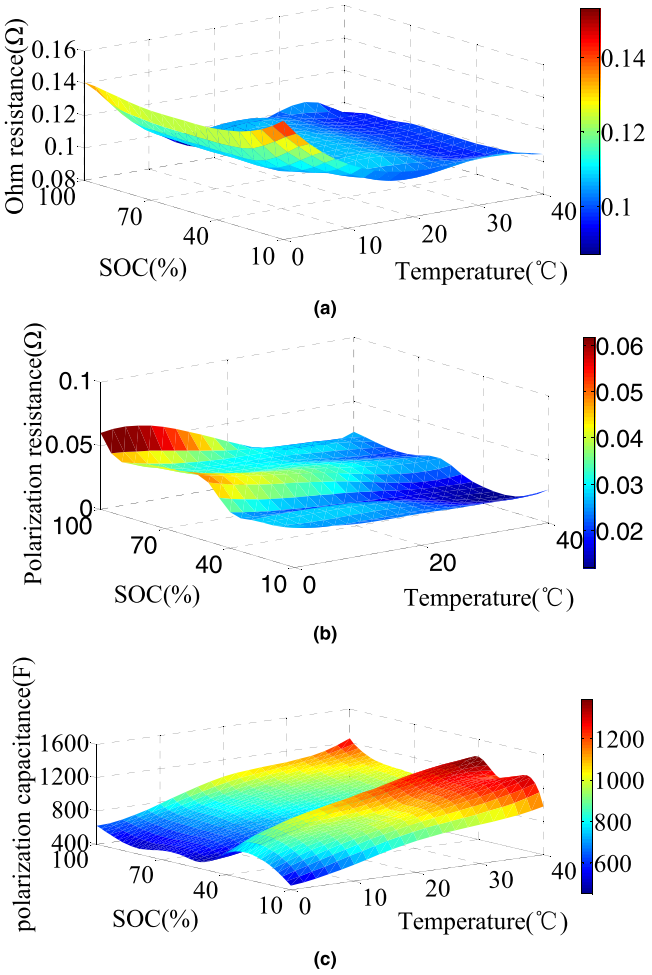

FIGURE 7. Battery parameter identification results: (a) R_0-SOC-T. (b) R_p-SOC-T. (c) C_p-SOC-T.

respectively.

$$e_t = \frac{|U_{measuerd,t} - U_{simulation,t}|}{U_{measuerd,t}} \times 100\% \quad (2)$$

$$MAE = \frac{1}{n}\sum_{t=1}^{n} |e_t| \quad (3)$$

Fig. 9 and Table 2 show that under different ambient temperatures, the errors between the measured voltage and the estimated voltage are very small, which are within 1.5%, and the average absolute errors are within 0.3%, which indicates that the model accuracy is satisfactory [7]. The simulation results show that the Thevenin equivalent circuit model can accurately reflect the battery dynamics.

In order to further verify the adopted battery model, DST verification is performed at 25°C, since the battery capacity, open-circuit voltage, ohm resistance, polarization resistance, and polarization capacitance are unknown and spline-interpolated [35] by the parameters at 20°C and 30°C.

As shown in Fig. 10, at 25°C, the error of the voltage estimation is very small, which is below 1%, and the average absolute error is 0.2551%. The accuracy of the

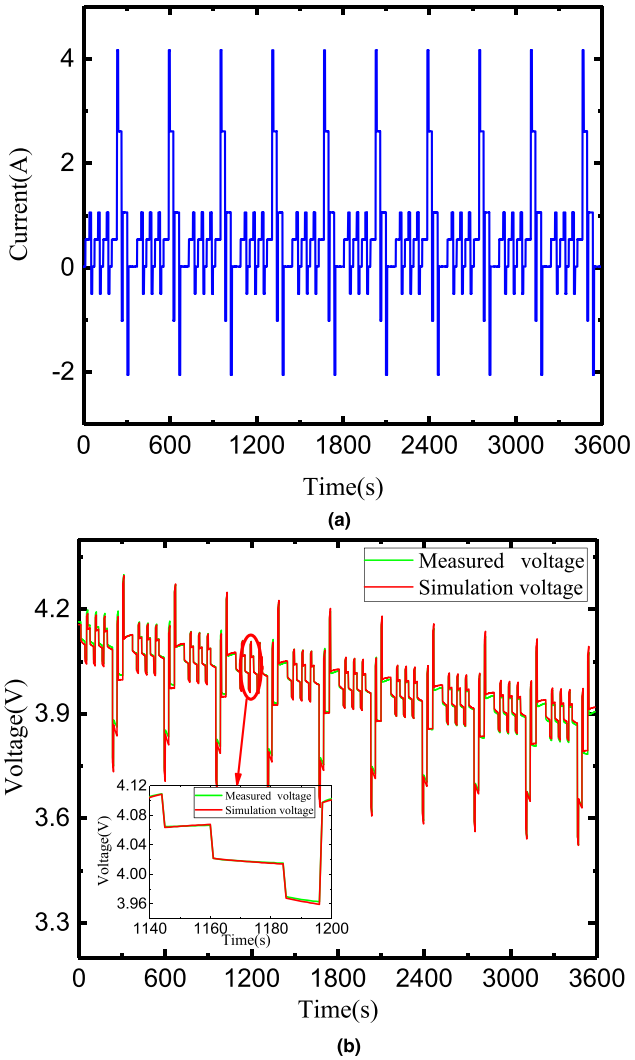

FIGURE 8. 20°C, Equivalent Circuit Model Verification Results Under. DST: (a) DST current. (b) Simulation voltage and the measured voltage.

Thevenin equivalent circuit model with temperature compensation established in this paper is therefore verified. As a result, the battery SOC can be estimated based on this model.

III. BATTERY SOC ESTIMATION

The standard Kalman Filter is a digital filtering algorithm based on the minimum mean square variance, which is applicable to the linear systems, where the error conforms to the Gaussian distribution system. However, in practice, many systems are nonlinear, and the standard Kalman Filter algorithm cannot provide satisfactory results. In this case, a straightforward solution is to linearize the system. The EKF algorithm [36] is based on the general nonlinear system, and the nonlinear function is expanded into the Taylor series around the filter value and omit the items above second order. The linear model of the nonlinear system is obtained. Therefore, the EKF can only reach the first-order

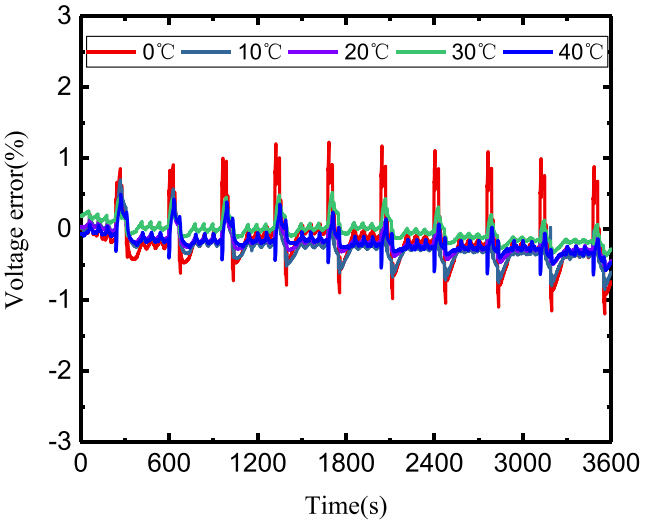

FIGURE 9. Simulation voltage and measured voltage error under DST.

Taylor series accuracy. it is difficult to achieve high accuracy for the system with strong nonlinearities. To improve the estimation performance, Julie proposed the UKF filtering method, which first performs U transformation when dealing with the state equation, and then uses the transformed state variables to reduce the estimation error. Because of the strong non-linear characteristics of the ternary polymer lithium-ion battery, the UKF algorithm is used to estimate the SOC.

A. UKF ALGORITHM

The discrete nonlinear system dynamic equations can be described as the state equations and the observed equations given as

$$x_{k+1} = f(x_k, u_k) + w_k \tag{4}$$

$$y_k = g(x_k, u_k) + v_k \tag{5}$$

Where u_k is the state variable, u_k is the control variable, y_k is the observation variable, $f(x_k, u_k)$ is the nonlinear state transfer equation,$g(x_k, u_k)$ is the nonlinear observation equation. w_k is the noise of system, v_k is the noise of observed, assuming that $w_k$and v_k are independent Gaussian white noise with covariance matrices of Q and R, respectively. Set a nonlinear transformation

$$y = f(x) \tag{6}$$

The U transform is based on the mean $\bar{x}$ and variance P_x of the current state x and constructs a series of Sigma points. We calculate its non-linear transformation for the Sigma point and obtain $\bar{y}$ and P_z. Usually, the number of Sigma points is $2n+1$, where n is the number of state variables.

The specific process of U transformation can be described as follows:

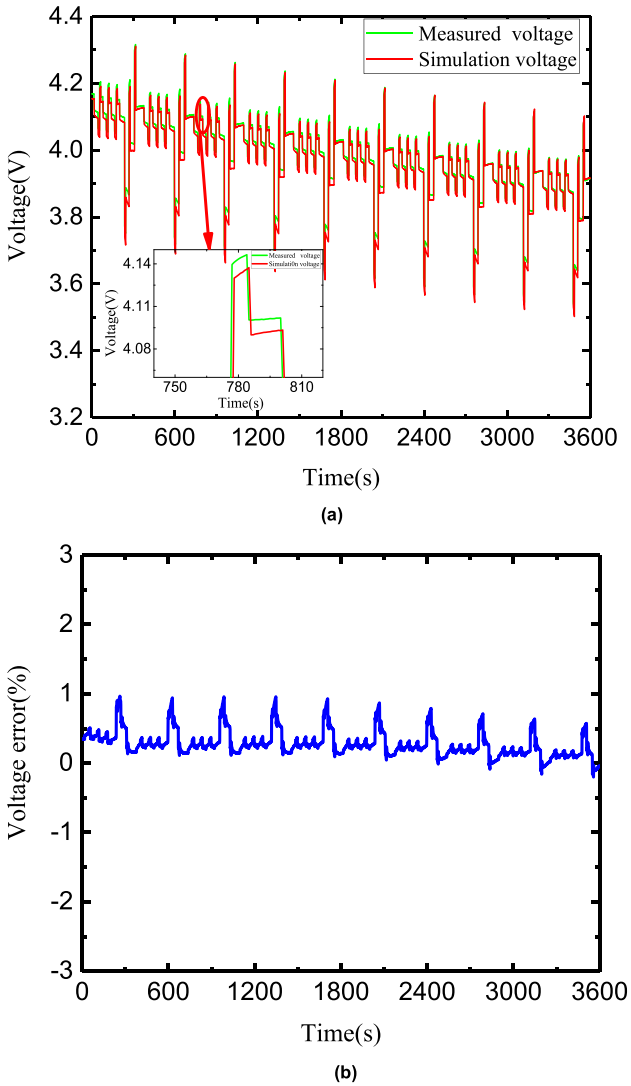

FIGURE 10. 25°C, Equivalent circuit model verification results under DST: (a) Voltage comparison. (b) Voltage error.

1) Construct the Sigma point and the weight value.

$2n+1$ sigma points are constructed and the corresponding weighting coefficients as

$$\begin{cases} \chi_0 = \widehat{x}, & i = 0 \\ \chi_i = \widehat{x} + \left(\gamma\sqrt{P_x}\right)_{(i)}, & i = 1, 2, \ldots, n-1, n \\ \chi_i = \widehat{x} - \left(\gamma\sqrt{P_x}\right)_{(i)}, & i = n+1,\ n+2, \ldots 2n-1, 2n \end{cases} \tag{7}$$

$$\begin{cases} w_0^{(m)} = \dfrac{\lambda}{n+\lambda} \\ w_0^{(c)} = \dfrac{\lambda}{n+\lambda} + \left(1-\alpha^2+\beta\right) \\ w_i^{(m)} = w_i^{(c)} = \dfrac{1}{2\left(n+\lambda\right)}, \quad i = 1, 2, \ldots 2n \end{cases} \tag{8}$$

$$\lambda = \alpha^2\left(n+k\right) - n \tag{9}$$

In equations (7) - (10), $\gamma = \sqrt{n+\lambda}$; the coefficient α determines the distribution of the Sigma point, usually taking a small positive value; k usually takes 0; β is used to describe the distribution information of γ (for Gaussian noise, the optimal value is 2); $\left(\gamma\sqrt{P_x}\right)_{(i)}$ represents the square root of the matrix i-th column; $w_i^{(m)}(i = 0, 1, 2, \ldots 2n)$ denotes the first-order statistical characteristics of the weight coefficient; $w_i^{(c)}$ $(i = 0, 1, 2, \ldots 2n)$ denotes the second-order statistical characteristics of the weight coefficient.

2) The nonlinear propagation of the Sigma point is given by (10).

$$Y^{(i)} = f\left(\chi_i\right), \quad i = 0, 1, 2, .., 2n \tag{10}$$

3) The mean $\bar{y}$ and variance P_z are given by (11)-(12).

$$\bar{z} = \sum_{i=0}^{2n} w_i^{(m)} Y^{(i)} \tag{11}$$

$$P_z = \sum_{i=0}^{2n} w_i^{(c)} \left[Y^{(i)} - \bar{z}\right]\left[Y^{(i)} - \bar{z}\right]^T \tag{12}$$

For non-linear systems shown in (4) and (5), the specific steps for filtering with UKF are as follows:

1) Set the initial value as

$$\hat{x}_{(0)} = E\left[x_{(0)}\right], \quad P_{x(0)} = \left\{\left[x_{(0)} - \hat{x}_{(0)}\right]\left[x_{(0)} - \hat{x}_{(0)}\right]^T\right\} \tag{13}$$

2) Time update.

① When k > 1, according to (7), structure 2n + 1 Sigma points as (14).

$$\chi_{(k-1)} = \{\hat{x}_{(k-1)}, \hat{x}_{(k-1)} + \left[\gamma\sqrt{P_{x,(k-1)}}\right]_i, \times \hat{x}_{(k-1)} - \left[\gamma\sqrt{P_{x,(k-1)}}\right]_i\}\ (i = 1, 2, \ldots, n) \tag{14}$$

② Calculate the prediction of Sigma points as

$$\chi_{i,k} = f\left[\chi_{i,k-1}\right], \quad (i = 1, 2, \ldots, 2n) \tag{15}$$

③ Calculate the mean and variance of the predicted Sigma point as

$$\widehat{x}_{(k+1,k)} = \sum_{i=0}^{2n} w_i^{(m)} \chi_{i,(k+1,k)} \tag{16}$$

$$P_{x,k}^{-} = \sum_{i=0}^{2n} w_i^{(c)} \left[\chi_{i,(k+1,k)} - \hat{x}_{(k+1,k)}\right] \times \left[\chi_{i,(k+1,k)} - \hat{x}_{(k+1,k)}\right]^T + Q\left(k\right) \tag{17}$$

3) Measurement update as shown in equations (18) - (20).

$$x_{(k+1,k+1)} = x_{(k+1,k)} + K\left[z_{k+1,k} - \widehat{z}_{k+1,k}\right] \tag{18}$$

$$P_{x,k} = P_{x,k}^{-} - KP_{z,k}K^T \tag{19}$$

$$K = P_{xz,k}P_{z,k}^{-1} \tag{20}$$

In the equations

$$\widehat{z}_{k+1,k} = \sum_{i=0}^{2n} w_i^{(m)} g\left[\chi_{i,k}\right] \tag{21}$$

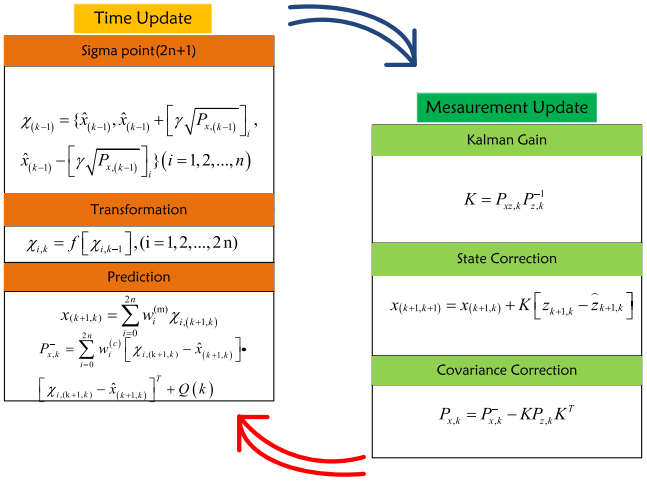

FIGURE 11. UKF algorithm flow chart.

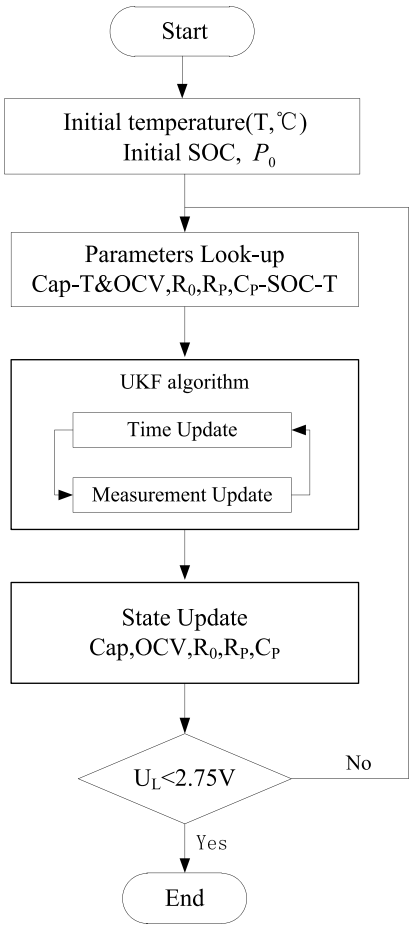

FIGURE 12. SOC estimation flow chart.

$$P_{z,k} = \sum_{i=0}^{2n} w_i^{(c)} \left\{ g\left(\chi_{i,k}\right) - \hat{z}_{k+1,k} \right\} \left\{ g\left(\chi_{i,k}\right) - \hat{z}_{k+1,k} \right\}^T + R\left(k\right) \tag{22}$$

$$P_{xz,k} = \sum_{i=0}^{2n} w_i^{(c)} \left\{ g\left(\chi_{i,k}\right) - x_{(k+1,k)} \right\} \left\{ g\left(\chi_{i,k}\right) - \hat{z}_{k+1,k} \right\}^T \tag{23}$$

The flowchart of UKF algorithm is depicted in Fig.11.

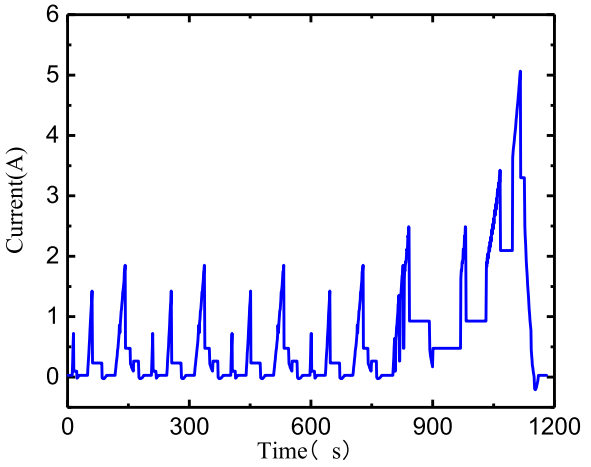

FIGURE 13. The NEDC current.

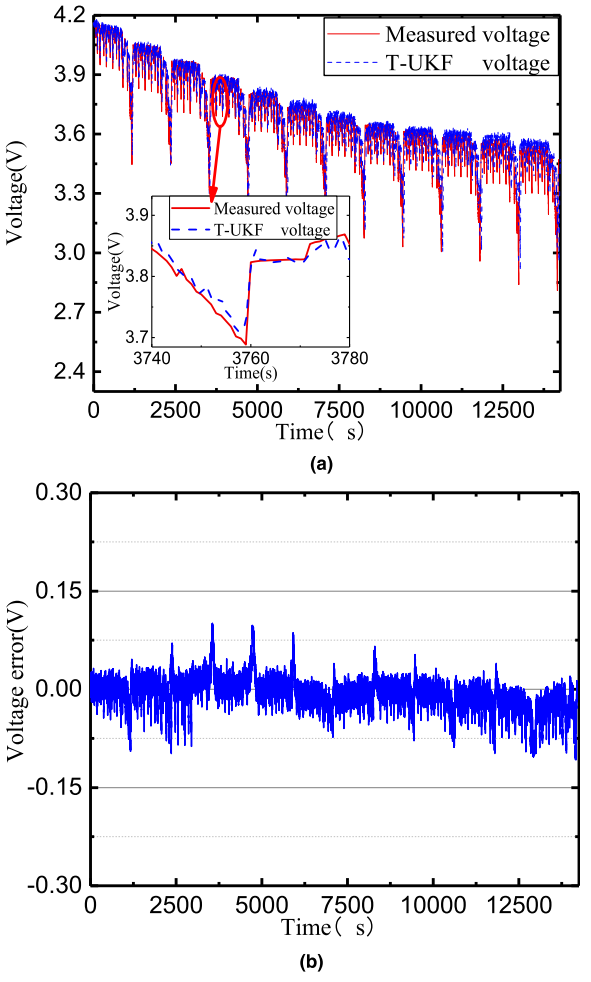

FIGURE 14. 20°C, T-UKF algorithm estimates voltage results: (a) Voltage comparison. (b) Voltage error.

B. SOC ESTIMATION BASED ON UNSCENTED KALMAN FILTERING ALGORITHM

The SOC expression is given by (24)[37].

$$SOC = SOC_0 - \frac{\int_0^t \eta \cdot Idt}{C} \tag{24}$$

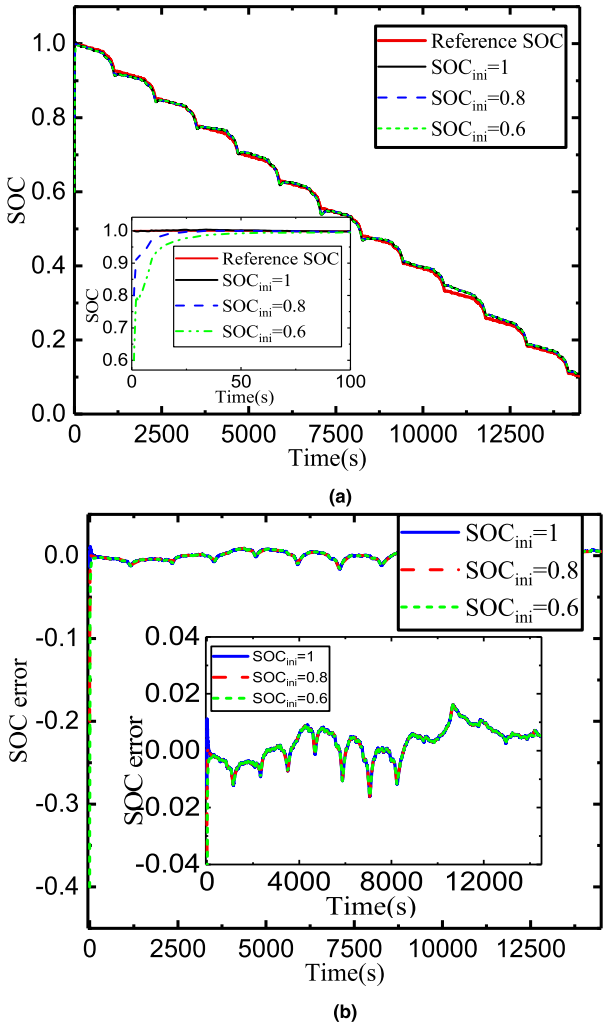

FIGURE 15. 20°C, the SOC estimation results of the proposed T-UKF method: (a) Comparison of reference SOC and estimated SOC with different initial SOC Initial value. (b) Error of reference SOC and estimated SOC.

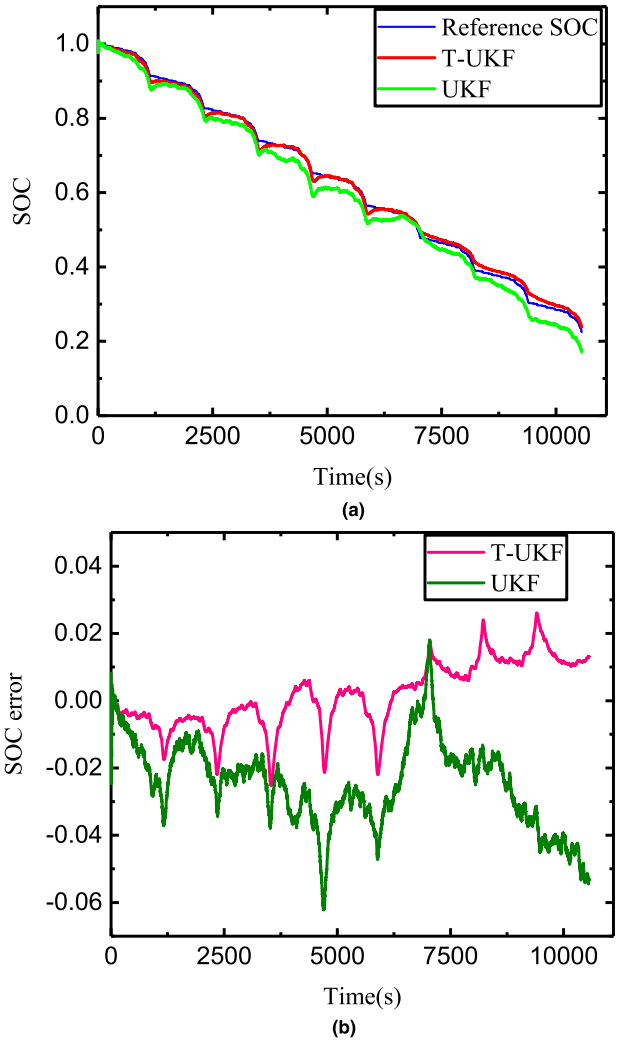

FIGURE 16. 0°C, SOC estimation results by T-UKF and UKF algorithms: (a) Comparison of two algorithms estimation results. (b) Error of two algorithms estimation.

Where η is charge-discharge efficiency, I_L is real-time current(when discharging, $I_L > 0$; when charging, $I_L < 0$), C is the battery rated capacity.

The equation (24) is discretized using the sampling time Δt to obtain equation (25). In this paper, $\Delta t = 1s$.

$$SOC_k = SOC_{k-1} - \eta \cdot I_{L,k} \Delta t / C \tag{25}$$

According to the SOC definition and the circuit equ-ation of the battery model, we can obtain the discrete space state of the battery model as shown in (26).

$$\begin{cases} SOC_k = SOC_{k-1} - \eta \cdot I_{L,k} \Delta t / C \\ U_{p,k} = U_{p,k-1} \exp\left(-\dfrac{\Delta t}{C_p R_p}\right) + I_{L,k-1} \\ \qquad \cdot R_p \left(1 - \exp\left(-\dfrac{\Delta t}{C_p R_p}\right)\right) \end{cases} \tag{26}$$

In the equation

$$\tau(\mathrm{SOC,T}) = \mathrm{C}_p(\mathrm{SOC,T}) \cdot R_p(\mathrm{SOC,T}) \tag{27}$$

Define the state variable as (28)

$$x_k = \left(SOC_k, U_{p,k}\right)^T \tag{28}$$

The observation equation is shown in (29)

$$U_{L,k} = U_{oc}\left(SOC_k, T\right) - I_{L,k} R_0(SOC_k, T) - U_{p,k} \tag{29}$$

Define the observed variable as

$$y_k = U_{L,k} \tag{30}$$

In summary, the SOC estimation flow chart is shown as Fig.12.

IV. SIMULATION AND EXPERIMENTAL RESULTS ANALYSIS

In order to verify the effectiveness of the proposed method, the paper uses the NEDC [38] to estimate the SOC of the battery. The UKF algorithm based on the temperature compensation model is denoted as T-UKF, and the T-UKF algorithm runs according to the flow of Fig.12. The parameter

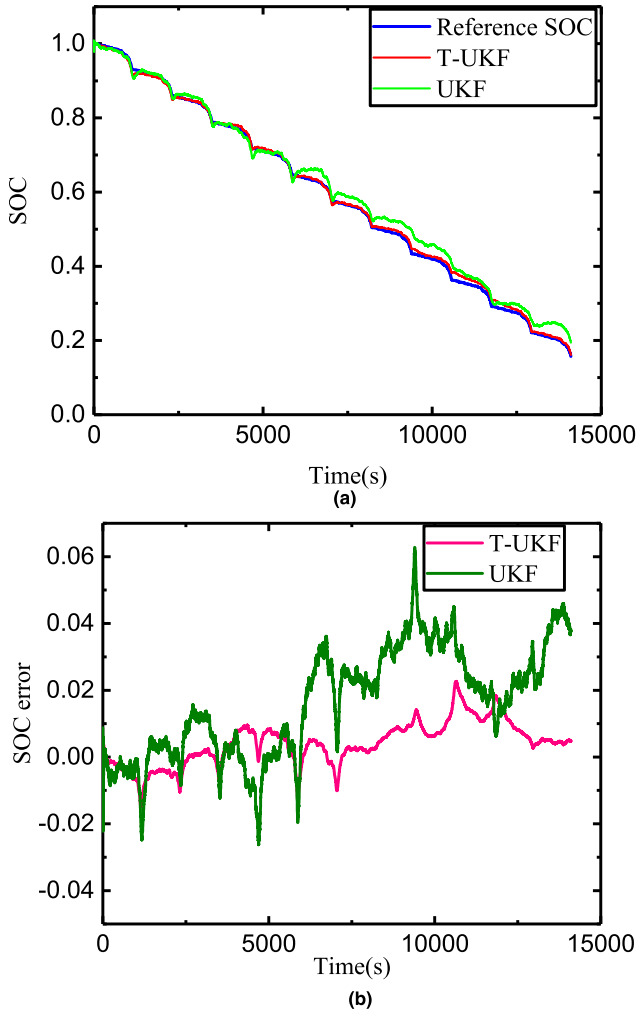

FIGURE 17. 40°C, SOC estimation results by T-UKF and UKF algorithms: (a) Comparison of two algorithms estimation results. (b) Error of two algorithms estimation.

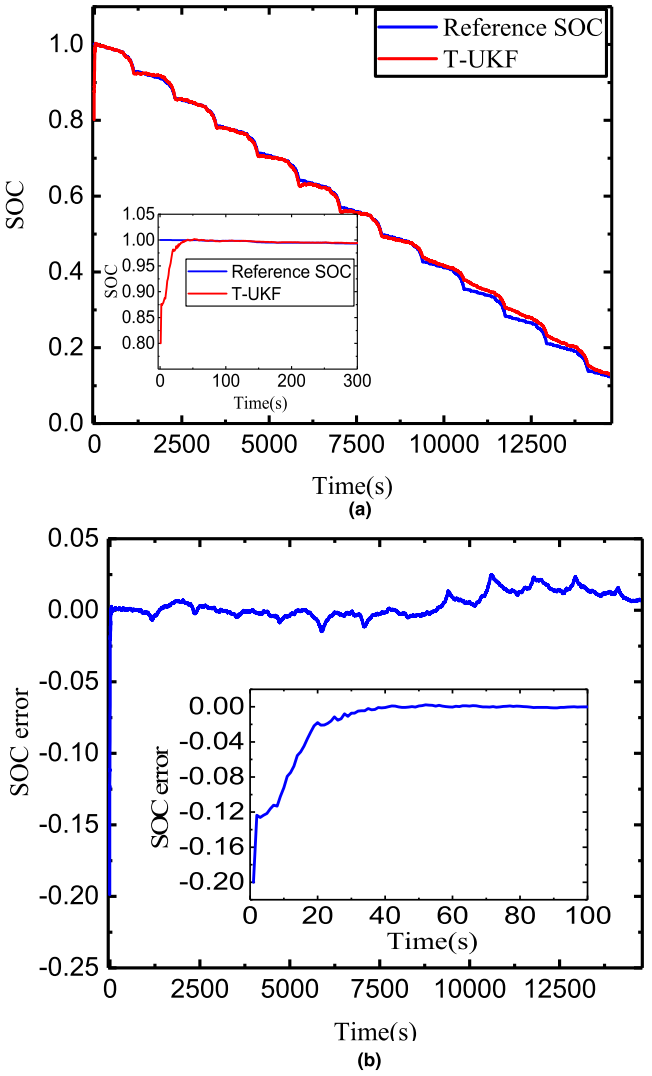

FIGURE 18. 25°C, the SOC estimation results by the proposed T-UKF method: (a) Comparison of reference SOC and estimated SOC. (b) Error reference SOC and of estimated SOC.

initialization of the T-UKF algorithm is given by

$$x_0 = \begin{bmatrix} 1 \\ 0 \end{bmatrix}, \quad P_0 = \begin{bmatrix} 0.01 & 0 \\ 0 & 0.01 \end{bmatrix} \tag{31}$$

In this paper, 25% of the braking energy is considered to charge the battery [39]. The NEDC current is shown in Fig. 13.

This paper used the proposed T-UKF algorithm to estimate the battery SOC. Fig. 14 shows the estimated voltage and the estimation error under NEDC when the ambient temperature is 20°C. Fig. 14(b) shows that the maximum voltage estimation error of T-UKF algorithm is within 3%. According to the evaluation of [40], the T-UKF estimation algorithm can accurately reflect the voltage variation of the battery under various operating conditions.

To test the robustness of the proposed algorithm, various SOC initial values are set in the T-UKF algorithm. The SOC initial values are set to 80% and 60%. The actual initial SOC value of the battery is 100%.

As shown in Fig. 15, the proposed method quickly eliminated the initial SOC error and the estimated SOC converged to the reference SOC value within 100 s, although significant SOC initial errors exist, the maximum error of SOC estimation is within 0.02, which reveals a satisfactory SOC estimation performance. It is proved that T-UKF is robust and effective to accurately estimate the battery SOC.

To verify the effectiveness of the T-UKF algorithm over a wide temperature range, the SOC estimation was performed using the T-UKF and UKF algorithms under NEDC at 0°C and 40°C, respectively. The UKF algorithm based on the traditional OCV-SOC model uses battery parameters at room temperature of 20°C. The SOC estimation results are shown in Fig.16 and Fig. 17, which show that at 0°C and 40°C, the SOC estimation error is large when the UKF algorithm is used regardless of the temperature compensation, and the maximum error exceeds 6%. For the T-UKF algorithm proposed in this paper, SOC estimation can well converge to the

reference SOC value, and the maximum error is within 3%. It is illustrated that the T-UKF algorithm proposed in this paper achieves a dramatic improvement in SOC estimation under various temperature.

To further verify the adaptability of the proposed T-UKF algorithm at different temperatures, the test is also performed at 25°C, where the battery parameters are unknown and obtained by spline interpolation based on the parameters at 20°C and 30°C. The T-UKF algorithm is used to estimate the battery SOC under NEDC. The true initial value of SOC is 100%. In the estimation algorithm, the initial value of SOC was set to 80%, as shown in Fig. 18. The estimated SOC quickly converges to the reference value when the proposed algorithm is adopted. The estimation error of battery SOC is consistently within 3% and the average error is controlled below 1%. It is demonstrated that accurate SOC estimation over a wide temperature range can be conducted by the proposed T-UKF algorithm.

V. CONCLUSION

In order to achieve accurate battery SOC estimation over a wide temperature range, a Thevenin equivalent circuit model with temperature compensation is proposed in this paper. Recursive least square method was used to identify the parameters of the battery, and the battery model is verified under DST. On this basis, a T-UKF estimation algorithm is proposed to achieve accurate SOC estimation considering the parameters variations under different temperatures. In this paper, T-UKF was compared with the UKF algorithm under NEDC in the experiments, and the advantages of the proposed T-UKF algorithm are mainly reflected in the following:

(1) The battery SOC estimation error caused by the ambient temperature can be effectively reduced, and the SOC estimation accuracy under various temperature conditions is significantly improved when compared with the conventional UKF algorithm, and the SOC estimation error is reduced by 3%.

(2) When the proposed T-UKF algorithm is adopted, the SOC estimation value can quickly converge to the reference value even if the significant initial SOC errors exist, and the SOC estimation errors are below 3%.

REFERENCES

[1] F. Sun, R. Xiong, and H. He, "Estimation of state-of-charge and state-of-power capability of lithium-ion battery considering varying health conditions," *J. Power Sources*, vol. 259, pp. 166–176, Aug. 2014.

[2] M. Dubarry, N. Vuillaume, and B. Y. Liaw, "From single cell model to battery pack simulation for Li-ion batteries," *J. Power Sources*, vol. 186, no. 2, pp. 500–507, 2009.

[3] X. Gong, R. Xiong, and C. C. Mi, "Study of the characteristics of battery packs in electric vehicles with parallel-connected lithium-ion battery cells," *IEEE Trans. Ind. Appl.*, vol. 51, no. 2, pp. 1872–1879, Mar./Apr. 2015.

[4] R. Xiong, J. Cao, Q. Yu, H. He, and F. Sun, "Critical review on the battery state of charge estimation methods for electric vehicles," *IEEE Access*, vol. 6, pp. 1832–1843, 2018.

[5] H. He, R. Xiong, and J. Fan, "Evaluation of lithium-ion battery equivalent circuit models for state of charge estimation by an experimental approach," *Energies*, vol. 4, no. 4, pp. 582–598, 2011.

[6] R. Xiong, H. He, F. Sun, X. Liu, and Z. Liu, "Model-based state of charge and peak power capability joint estimation of lithium-ion battery in plug-in hybrid electric vehicles," *J. Power Sour.*, vol. 229, pp. 159–169, May 2013.

[7] Y. Tian, B. Xia, W. Sun, Z. Xu, and W. Zheng, "A modified model based state of charge estimation of power lithium-ion batteries using unscented Kalman filter," *J. Power Sources*, vol. 270, pp. 619–626, Dec. 2014.

[8] Y. Li, C. Wang, and J. Gong, "A combination Kalman filter approach for State of Charge estimation of lithium-ion battery considering model uncertainty," *Energy*, vol. 109, pp. 933–946, Aug. 2016.

[9] Y. Zhang, R. Xiong, and H. He, "Evaluation of the model-based state-of-charge estimation methods for lithium-ion batteries," in *Proc. IEEE Transp. Electrific. Conf. Expo (ITEC)*, 2016, pp. 1–8.

[10] M. A. Roscher and D. U. Sauer, "Dynamic electric behavior and open-circuit-voltage modeling of $LiFePO_4$-based lithium ion secondary batteries," *J. Power Sources*, vol. 196, no. 1, pp. 331–336, 2011.

[11] Z. Li, L. Lu, and M. Ouyang, "Comparison of methods for improving SoC estimation accuracy through an ampere-hour integeration approach," *J. Tsinghua Univ. (Sci. Technol.)*, vol. 50, no. 8, pp. 1293–1296, Aug. 2010.

[12] H. He, R. Xiong, X. Zhang, F. Sun, and J. Fan, "State-of-charge estimation of the lithium-ion battery using an adaptive extended Kalman filter based on an improved Thevenin model," *IEEE Trans. Veh. Technol.*, vol. 60, no. 4, pp. 1461–1469, May 2011.

[13] R. Xiong, J. Tian, H. Mu, and C. Wang, "A systematic model-based degradation behavior recognition and health monitoring method for lithium-ion batteries," *Appl. Energy*, vol. 207, pp. 372–383, Dec. 2017.

[14] R. Xiong, Y. Zhang, H. He, X. Zhou, and M. Pecht, "A double-scale, particle-filtering, energy state prediction algorithm for lithium-ion batteries," *IEEE Trans. Ind. Electron.*, vol. 65, no. 2, pp. 1526–1538, Feb. 2018.

[15] R. Xiong, Q. Yu, L. Y. Wang, and C. Lin, "A novel method to obtain the open circuit voltage for the state of charge of lithium ion batteries in electric vehicles by using H infinity filter," *Appl. Energy*, vol. 207, pp. 346–353, Dec. 2017.

[16] Q. Yu, R. Xiong, C. Lin, W. Shen, and J. Deng, "Lithium-ion battery parameters and state-of-charge joint estimation based on H-infinity and unscented Kalman filters," *IEEE Trans. Veh. Technol.*, vol. 66, no. 10, pp. 8693–8701, Oct. 2017.

[17] L. Shulin, C. Naxin, L. Yan, and C. Zhang, "Modeling and state of charge estimation of lithium-ion battery based on theory of fractional order for electric vehicle," *Trans. China Electrotech. Soc.*, vol. 32, no. 4, pp. 189–194, Feb. 2017.

[18] H. Chaoui, C. C. Ibe-Ekeocha, and H. Gualous, "Aging prediction and state of charge estimation of a $LiFePO_4$ battery using input time-delayed neural networks," *Electr. Power Syst. Res.*, vol. 146, pp. 189–197, May 2017.

[19] F. Feng, R. Lu, and C. Zhu, "A combined state of charge estimation method for lithium-ion batteries used in a wide ambient temperature range," *Energies*, vol. 7, no. 5, pp. 3004–3032, May 2014.

[20] F. Feng, R. Lu, G. Wei, and C. Zhu, "Online estimation of model parameters and state of charge of $LiFePO_4$ batteries using a novel open-circuit voltage at various ambient temperatures," *Energies*, vol. 8, no. 4, pp. 2950–2976, 2015.

[21] X. Liu, Z. Chen, C. Zhang, and J. Wu, "A novel temperature-compensated model for power Li-ion batteries with dual-particle-filter state of charge estimation," *Appl. Energy*, vol. 123, pp. 263–272, Jun. 2014.

[22] K.-T. Lee, M.-J. Dai, and C.-C. Chuang, "Temperature-compensated model for lithium-ion polymer batteries with extended Kalman filter state-of-charge estimation for an implantable charger," *IEEE Trans. Ind. Electron.*, vol. 65, no. 1, pp. 589–596, Jan. 2018.

[23] Y. Xing, W. He, M. Pecht, and K. L. Tsui, "State of charge estimation of lithium-ion batteries using the open-circuit voltage at various ambient temperatures," *Appl. Energy*, vol. 113, pp. 106–115, Jan. 2014.

[24] K. S. Ng, C.-S. Moo, Y.-P. Chen, and Y.-C. Hsieh, "Enhanced coulomb counting method for estimating state-of-charge and state-of-health of lithium-ion batteries," *Appl. Energy*, vol. 86, no. 9, pp. 1506–1511, Sep. 2009.

[25] Y.-H. Chiang, W.-Y. Sean, and J.-C. Ke, "Online estimation of internal resistance and open-circuit voltage of lithium-ion batteries in electric vehicles," *J. Power Sour.*, vol. 196, no. 8, pp. 3921–3932, 2011.

[26] T. Bernd, M. Kleutges, and A. Kroll, "Nonlinear black box modelling—Fuzzy networks versus neural networks," *Neural Comput. Appl.*, vol. 8, no. 2, pp. 151–162, 1999.

[27] F. Sun, X. Hu, Y. Zou, and S. Li, "Adaptive unscented Kalman filtering for state of charge estimation of a lithium-ion battery for electric vehicles," *Energy*, vol. 36, no. 5, pp. 3531–3540, 2011.

[28] C. Lin, B. Qiu, and Q. Chen, "A comparative study on power input equivalent circuit model for electric vehicle battery," *Automot. Eng.*, vol. 28, pp. 229–234, 2006.
[29] X. Hu, S. Li, and H. Peng, "A comparative study of equivalent circuit models for Li-ion batteries," *J. Power Sour.*, vol. 198, pp. 359–367, Jan. 2012.
[30] H. He, R. Xiong, H. Guo, and S. Li, "Comparison study on the battery models used for the energy management of batteries in electric vehicles," *Energy Convers. Manage.*, vol. 64, pp. 113–121, Dec. 2012.
[31] H. Chaoui and H. Gualous, "Adaptive state of charge estimation of lithium-ion batteries with parameter and thermal uncertainties," *IEEE Trans. Control Syst. Technol.*, vol. 25, no. 2, pp. 752–759, Mar. 2017.
[32] T. Zahid and W. Li, "A comparative study based on the least square parameter identification method for state of charge estimation of a $LiFePO_4$ battery pack using three model-based algorithms for electric vehicles," *Energies*, vol. 9, no. 9, p. 720, 2016.
[33] J. Lindgren and P. D. Lund, "Effect of extreme temperatures on battery charging and performance of electric vehicles," *J. Power Sources*, vol. 328, pp. 37–45, Oct. 2016.
[34] R. Xiong, H. He, F. Sun, and K. Zhao, "Evaluation on state of charge estimation of batteries with adaptive extended Kalman filter by experiment approach," *IEEE Trans. Veh. Technol.*, vol. 62, no. 1, pp. 108–117, Jan. 2013.
[35] M. Ghasemi, "On using cubic spline for the solution of problems in calculus of variations," *Numer. Algorithms*, vol. 73, no. 3, pp. 685–710, 2016.
[36] G. L. Plett, "Extended Kalman filtering for battery management systems of LiPB-based HEV battery packs: Part 1. Background," *J. Power Sources*, vol. 134, no. 2, pp. 252–261, 2004.
[37] S. Yuan, H. Wu, and C. Yin, "State of charge estimation using the extended Kalman filter for battery management systems based on the ARX battery model," *Energies*, vol. 6, no. 1, pp. 444–470, 2013.
[38] C. Dextreit and I. V. Kolmanovsky, "Game theory controller for hybrid electric vehicles," *IEEE Trans. Control Syst. Technol.*, vol. 22, no. 2, pp. 652–663, Mar. 2014.
[39] A. Tourani, P. White, and P. Ivey, "Analysis of electric and thermal behaviour of lithium-ion cells in realistic driving cycles," *J. Power Sources*, vol. 268, pp. 301–314, Dec. 2014.
[40] R. Xiong, X. Gong, C. C. Mi, and F. Sun, "A robust state-of-charge estimator for multiple types of lithium-ion batteries using adaptive extended Kalman filter," *J. Power Sources*, vol. 243, pp. 805–816, Dec. 2013.

XIAOGANG WU was born in Hegang, Heilongjiang, China. He received the M.E. and Ph.D. degrees in power electronics and power transmission from the Harbin University of Science and Technology, Harbin, China, in 2006 and 2009, respectively. He studied at Tsinghua University in Beijing, China, from 2010 to 2012 as a Postdoctoral Researcher.

He is currently a Professor with the Harbin University of Science and Technology. His research mainly focuses on optimization matching and energy management of hybrid power system, power battery charge management, and electric vehicle access technology.

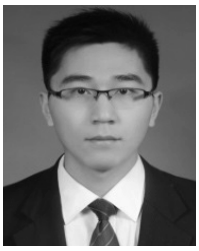

XUEFENG LI was born in Weifang, Shandong, China. He received the B.E. degree in electrical engineering and automation from the Qingdao University of Technology, Qingdao, China, in 2014. He is currently pursuing the M.E. degree in electrical engineering with the Harbin University of Science and Technology, Harbin, China.

His research mainly focuses on the battery management system in electric vehicles.

JIUYU DU received the Ph.D. degree from the School of Mechanical Engineering, Beijing Institute of Technology, Beijing, China, in 2009. She studied at Tsinghua University in Beijing, China, from 2009 to 2012 as a Postdoctoral Researcher.

She is currently an Assistant Researcher with the Department of Automotive Engineering, Tsinghua University. Her research mainly focuses on power battery management and electric vehicle technology.